A gel-coated air-liquid-interface culture system with tunable 1 substrate stiffness matching healthy and diseased lung 2 tissues 3 Zhi-Jian He^{3,†}, Catherine Chu^{1,†}, Riley Dickson², Kenichi Okuda⁴, Li-Heng Cai^{1,2,3,*} 4 5 ¹Soft Biomatter Laboratory, Department of Materials Science and Engineering, University of 6 Virginia, Charlottesville, VA 22904, USA 7 8 ²Department of Chemical Engineering, University of Virginia, Charlottesville, VA 22904, US 9 10 ³Department of Biomedical Engineering, University of Virginia, Charlottesville, VA 22904, 11 USA 12 ⁴Marsico Lung Institute/Cystic Fibrosis Research Center, University of North Carolina at Chapel 13 Hill, Chapel Hill, NC 27599, USA 14 15 16 * Corresponding author. Email: liheng.cai@virginia.edu 17 † Equal contribution 18 19 20 Corresponding author contact: 21 Dr. Li-Heng Cai 22 228 Wilsdorf Hall 23 University of Virginia 395 McCormick Road 24 25 Charlottesville, VA 22904 26 Tel: 434-924-2512 27 Fax: 434-982-5660 28 29 **Supplementary Material and Movies available at:** 30 31 https://doi.org/10.6084/m9.figshare.24450193.v1

Abstract: Since its invention in the late 1980s, the air-liquid-interface (ALI) culture system has been the standard *in vitro* model for studying human airway biology and pulmonary diseases. However, in a conventional ALI system, cells are cultured on a porous plastic membrane that is much stiffer than human airway tissues. Here, we develop a gel-ALI culture system by simply coating the plastic membrane with a thin layer of hydrogel with tunable stiffness matching that of healthy and fibrotic airway tissues. We determine the optimum gel thickness that does not impair the transport of nutrients and biomolecules essential to cell growth. We show that the gel-ALI system allows human bronchial epithelial cells (HBECs) to proliferate and differentiate into pseudostratified epithelium. Further, we discover that HBECs migrate significantly faster on hydrogel substrates with stiffness matching that of fibrotic lung tissues, highlighting the importance of mechanical cues in human airway remodeling. The developed gel-ALI system provides a facile approach to studying the effects of mechanical cues in human airway biology and in modeling pulmonary diseases.

- **Keywords:** air-liquid-interface; substrate stiffness; human bronchial epithelia; cell differentiation; collective cell migration
- New and Noteworthy: In a conventional air-liquid-interface (ALI) system, cells are cultured on a plastic membrane that is much stiffer than human airway tissues. We develop a gel-ALI system by coating the plastic membrane with a thin layer of hydrogel with tunable stiffness matching that of healthy and fibrotic airway tissues. We discover that human bronchial epithelial cells migrate significantly faster on hydrogel substrates with pathological stiffness, highlighting the importance of mechanical cues in human airway remodeling.

1. Introduction

Cell culture models allow for recapitulating essential biological features of human organs or tissues, and thus represent powerful tools for studying cell biology, disease modeling, and drug discovery. For instance, air-liquid interface (ALI) culture system was developed in the late 1980s to study human airway biology and to model pulmonary diseases (1). In an ALI system, human bronchial epithelial cells (HBECs) are cultured on a porous membrane, through which nutrients are transported from cell culture media at the basal side, whereas on the apical side cells are in contact with air (2). The ALI system allows airway basal cells to differentiate into ciliated cells and goblet cells, eventually forming pseudostratified columnar epithelium that recapitulates essential biological features of the human airway epithelium (3–6) (Fig. 1a). Thus, since its invention the ALI culture system represents the standard *in vitro* model for studying human airway defense (7, 8), airway biology (9, 10), airway remodeling (11, 12), airway infection (13, 14), and muco-obstructive lung diseases (15) that include chronic obstructive pulmonary disease (COPD) (16), cystic fibrosis (17, 18), primary ciliary dyskinesia (19), and non-cystic fibrosis bronchiectasis (20).

The classical ALI culture system, however, suffers from two major limitations. *First*, the porous membrane is made of plastics such as polyester or polyethylene terephthalate, which has a shear modulus on the order of 10^9 Pa, $\sim 10^6$ times higher than that of human airway tissues. By contrast, in the human airway, epithelial cells are supported by extracellular matrix (ECM), which not only provides structural support and mechanical stability to the airway epithelium, but also serves as a microenvironment to regulate cell behavior and function (21, 22). For example, substrates with ECM mimicking stiffness affect the morphology of alveolar epithelial cells (23),

as well as the size of focal adhesions and the actin cytoskeleton (24). *Second*, the stiffness of the plastic membrane is nearly fixed and cannot be changed. By contrast, the stiffness of the lung tissues varies with pulmonary injuries or diseases (25). In idiopathic pulmonary fibrosis (IPF), a progressive lung disease of unknown causes that is characterized by dysregulated lung remodeling resulting in massive ECM production, the human lung tissues are stiffened from 0.6-1.5 kPa in health to 3-16 kPa in shear modulus in disease (26–29). Thus, the stiff plastic membrane intrinsically limits the applicability of the classical ALI system in studying the effects of ECM mechanical properties on airway epithelial cell behavior and function.

To better recapitulate the mechanical environment of lung tissues, various materials and methods have been developed to replace or coat the plastic membrane of the classical ALI system. For example, an elastomeric polydimethylsiloxane (PDMS) membrane can be used to separate two microfluidic channels, creating an ALI system for HBEC culture. Because the elastomeric membrane can be reversely deformed under stress, the microfluidic device, or lung-on-a-chip, provides a powerful platform for mimicking the cyclic mechanical strain of the lung alveolar barrier during breathing (30). Moreover, recently the same lung-on-a-chip concept was successfully extended to culture small airway cells (31). However, because PDMS elastomers are not permeable to water and nutrients, microscale pores must be introduced to the elastomeric membrane, making the lung-on-a-chip system dependent on multi-step, sophisticated microfabrication (32). Additionally, the stiffness of typical PDMS elastomers (33) is much higher than that of healthy and fibrotic lung tissues (34). Unlike elastomers, hydrogels are porous networks that allow for good nutrient transport and are very soft, with stiffness tunable in a wide range that can precisely match that of various tissues (35, 36). As a result, the hydrogel is a

promising candidate for substituting the plastic membrane in the ALI culture system. For example, an ALI magnetic microboat culture system has recently been developed (37), in which a layer of polyacrylamide (PAAm) hydrogel is integrated into silicone rings. Because of the buoyance of the silicone rings, the system rises to the liquid surface to form an ALI yet can be magnetically sunk to submerged culture. However, the operation of the microboat ALI culture system requires careful manipulation of the magnetic field. Additionally, the reported PAAm hydrogel thickness is 750 μ m, which is much larger than the typical upper limit of 200 μ m for sufficient nutrient transport for cell growth (38). Consequently, there is a need for a facile and robust ALI culture system with tunable substrate stiffness matching that of healthy and diseased lung tissues.

Here, we design and fabricate an *in vitro* culture system by coating a thin layer of PAAm hydrogel with a thickness of 100 µm onto the classical ALI culture system, as schematically illustrated in **Fig. 1b**. The stiffness of PAAm hydrogel can be precisely controlled to match that of healthy and fibrotic airway tissues. We determine the optimum gel thickness that does not impair the transport of nutrients and biomolecules essential to cell growth. Similar to the conventional ALI system, the gel-ALI system allows HBECs to proliferate and differentiate into pseudostratified epithelium, capturing the essential biological features *in vivo*. Using the gel-ALI system, we reveal that hydrogel substrates with pathologically relevant stiffness promote the migration of airway epithelial cells, highlighting the importance of the mechanical environment for the behavior of cells. The developed gel-ALI system represents the simplest possible *in vitro* model that enables mimicking the mechanical environment of human lung tissues, providing a

platform for studying previously less explored mechanical cues in human airway biology and pulmonary diseases.

2. Materials and Methods

Fabrication and characterization of gel-ALI system. To synthesize polyacrylamide (PAAm) hydrogel with a prescribed stiffness, we prepare a reaction mixture mixing acrylamide solution (AAm, MilliporeSigma, Cat. No. A4058, 40% w/v), *N,N'*-methylenebisacrylamide solution (BIS, MilliporeSigma, Cat. No. M1533, 2% w/v), and deionized (DI) water (Millipore), following the recipe listed in **Table S1**. To initiate polymerization, a final concentration of 0.12% w/v ammonium persulfate (APS, MilliporeSigma, Cat. No. 248614) is added as the catalyst, and 1.2% v/v N,N,N',N'-tetramethylethylenediamine (TEMED, MilliporeSigma, Cat. No. T9281) as an initiator is added to the mixture. For example, to synthesize a PAAm gel with a shear modulus of 1 kPa, the volume ratio of AAm: BIS: Water: TEMED: APS is 100:100:776:12:12; for a 16 kPa hydrogel, the ratio is 200:200:526:12:12 (**Table S1**).

There are multiple commercial insert types made of various materials such as polycarbonate, poly (ethylene terephthalate) (PET) and polytetrafluoroethylene (PTFE), which have a slight difference in stiffness but are all plastics with shear modulus on the order of GPa. There exists a study showing that compared to PET insert, HBECs grown on the relatively soft PTFE membrane (39) form a thicker and more stratified cell layer (40). Yet, all these inserts allow the formation of well-differentiated, pseudostratified human airway epithelium. In this study, we use Transwell® insert (Corning, Cat. No. 3401) made of polycarbonate, which has a shear modulus of 0.7 GPa (41). To coat a Transwell® insert with a PAAm hydrogel layer of 100 µm thickness,

we quickly apply 30 μL of the reaction mixture to the center of the Transwell[®] insert. In parallel, we prepare a circular coverslip of 11 mm in diameter by punching three layers of Scotch[®] tape and use the coverslip to spread the reaction mixture. Because the coverslip is hydrophobic and has a diameter slightly smaller than that of the Transwell[®] insert which is 12 mm, this process flattens the gel surface, and importantly, prevents the reaction mixture from oxygen, which is known to impair free radical polymerization. After 30 min, the coverslip is removed by a syringe with a curved needle tip, leaving a thin layer of hydrogel with the prescribed thickness. Afterward, the gel is rinsed using sterilized DI water. We seal 12-well plates containing gel-coated Transwell[®] inserts by parafilm and store them at 4 °C for future usage.

To quantify the gel thickness, we add 50 μ g/mL fluorescein isothiocyanate (FITC)-labeled dextran with a molecular weight of 70 kDa (Invitrogen, Cat. No. D1823) to the reaction mixture.

The gel thickness is quantified by measuring the thickness of the fluorescent region.

Rheological characterization of polyacrylamide hydrogel. We prepare a gel disk for rheological measurements. To do so, we add 800 μL reaction mixture to a well in a 12-well culture plate and cover the solution using a circular glass coverslip of 21 mm in diameter. After 30 min, the coverslip is removed, leaving a gel layer of ~2 mm in thickness. Form the gel layer, we cut a disk of 8 mm in diameter, load it to a stress-controlled rheometer (Anton Paar, MCR 302) with a plate-plate geometry of 8 mm in diameter, and cover the gel peripheral with mineral oil to avoid evaporation. We quantify the dynamic mechanical properties using oscillatory shear measurements at a fixed strain of 0.5 % but various frequency of 0.1 rad/sec to 100 rad/sec. Within the frequency range explored, the shear storage modulus is nearly independent of the

shear frequency. Therefore, we take the shear storage modulus at the lowest shear frequency, 0.1 rad/sec, as the equilibrium shear modulus G of the gel.

Measurement of transport properties gel-ALI system. We label the gel by premixing the reaction mixture with 70 kDa FITC-labeled dextran at a concentration of 50 μg/mL. The gel-ALI system is fabricated following the same protocol described above. We add DI water to the apical chamber of the Transwell[®] insert and monitor the fluorescence intensity using a fluorescence confocal microscope (Leica, SP8). The fluorescence intensity is quantified and normalized to the value at the initial time point.

Cell culture. We coat all ALI systems with type IV collagen for HBEC culture. For the conventional ALI system without gel, we coat the Transwell® insert following a previously established protocol (2). To coat the gel-ALI system, we activate the gel surface by sulfosuccinimidyl 6-(4'-azido-2'-nitrophenylamino) (sulfo-SANPAH, Thermo Scientific, Cat. No. 22589), which allows covalent conjugation of type IV collagen to the gel surface (42). Specifically, to each gel-coated Transwell® insert we add 100 μL of 2 mg/mL sulfo-SANPAH (MilliporeSigma, Cat. No. D2650) solution in DI water, expose the solution to UV light (37 mW, 365 nm) for 5 min to activate the gel surface, and then rinse the gel using DI water. For each well with activated gel surface, we add 150 μL of 0.005 mg/mL type IV collagen (MilliporeSigma, Cat. No. C7521) solution in DI water and store the gel-ALI system at 4 °C overnight to ensure adequate collagen coating. Then, the gel is sterilized by UV light for 15 min and ready for cell culture.

Primary HBECs (P0) are obtained from Marsico Lung Institute Tissue Procurement and Cell Culture Core at the University of North Carolina at Chapel Hill (UNC) under a protocol number 03-1396 approved by the UNC Biomedical Institutional Review Board. Cells from five normal donors 49/Female/Caucasian/Nonsmoker (NS);17/Male/Caucasian/NS; are used: 30/Female/Hispanic/NS; 27/Female/Caucasian/NS; 22/Female/Caucasian/NS. The primary cells are passaged using in a 100 mm tissue culture-treated culture dish (Corning 430167) using expansion medium (PneumaCultTM-Ex Plus Medium, STEMCELL Technologies, Cat. No. 05040). When cells reach >90% confluence, we passage the cells using accutase (Innovative Cell Technologies AT104, Cat. No. NC9839010). For all experiments, we use passage 2 (P2) cells, beyond which the HBECs may lose their stemness (2). We seed HEBCs at the density of 4.2×10^4 cells/insert and add expansion medium to both the basal and apical chambers. After 5-7 days, HBECs reach over 90% confluence. We transition the cultures to ALI by removing the apical medium and replacing the expansion medium with ALI culture media (PneumaCultTM-ALI Medium, STEMCELL Technologies, Cat. No. 05001). After 2 weeks of ALI culture, mucus starts to accumulate and is washed three times per week. To wash off mucus, to each insert we add 500 µL of Dulbecco's phosphate-buffered saline (DPBS, Gibco 14-200-075), incubate the cell culture for 15 min, and aspirate the DPBS in the apical chamber. The washing process is repeated three times.

209

210

211

212

213

191

192

193

194

195

196

197

198

199

200

201

202

203

204

205

206

207

208

Immunofluorescence microscopy. We use immunofluorescence staining to label the cells in a well-differentiated HBEC culture. To prepare for the staining, for each Transwell[®] we wash the culture three times using DPBS; for each washing, 500 μL of DPBS is added to the apical chamber and the culture is incubated at 37 °C for 20 min. After washing, we add 1 mL of 4%

w/v paraformaldehyde (Thermo Scientific, Cat. No. AA47392-9M) to the apical side of the Transwell® and incubate the culture at room temperature (RT) for 15 min to fix the cells. Then, we add 1 mL of 0.2% v/v Triton X-100 solution (Thermo Scientific, Cat. No. AAA16046AP) and incubate the culture at RT for 30 min to permeabilize the fixed cells. We add 1 mL of 3% (v/v) donkey serum (Abcam, Cat. No. AB7475) in DPBS solution and incubate the culture at RT for 1 hour; this process blocks non-specific binding of antibodies to cells.

220

221

222

223

224

225

226

227

228

229

230

231

232

233

234

235

214

215

216

217

218

219

For the above prepared cell culture, we use mouse anti-mucin 5AC (MUC5AC) antibody (ThermoFisher, Cat. No. MA5-12178) to label mucin granules in goblet cells and rabbit antiacetylated tubulin (AcTUB) antibody (Invitrogen, Cat. No. MA5-33079) to label tubulin in the cilia of ciliated cells. Specifically, 200 µL of primary antibody solution containing 10 µg/mL anti-MUC5AC antibody and 40 µg/mL of anti-AcTUB antibody is added to each well. The culture is maintained at 4 °C overnight to ensure the binding of the primary antibody to antigens. Afterward, we rinse the cell culture with DPBS three times and add to each well 200 µL of secondary antibody solution, which contains 10 µg/mL donkey anti-rabbit secondary antibody conjugated with Alexa Fluor 647 (Abcam, Cat. No. ab150075) and 10 µg/mL donkey anti-mouse secondary antibody conjugated with Alexa Fluor 488 (Abcam, Cat. No. ab150105). We incubate the culture at RT for 1 hour to allow the secondary antibodies to bind to the primary antibodies, and rinse the culture with DPBS three times afterward. After staining using secondary antibody, to each well we add 200 µL of 1 µg/mL 4',6-diamidino-2-phenylindole (DAPI, Invitrogen, Cat. No. D3571) solution in DI water, incubate the culture at RT for 5 min, and then wash the culture with DPBS three times. This process is to stain the cell nuclei.

To prepare the culture for imaging, we excise the Transwell® insert membrane, mount it on a glass cover slide, add about 1 mL FluorSave oil (MilliporeSigma, Cat. No. 345789) to completely cover the membrane, place a coverslip, and seal the edges of the coverslip using wax. We use multi-channel fluorescence confocal microscopy (Leica SP8) to image the cell culture. During imaging, we use sequential scan between frames to avoid the overlap of fluorescence from different channels. For each code of cell culture, we randomly select five regions of interest (ROIs) from five wells with one ROI from each well. We use five codes of cells from different normal donors to ensure sufficiently powered statistics. For each culture, we use a 10× dry objective to image a ROI with the dimension of 1162.5×1162.5 µm²; this allows us to image about 4000 cells/culture and a total number of ~10⁵ cells for each condition to avoid biased measurement of the cell population. To image the cilia of ciliated cells for the control sample, we use a 63× oil objective (numerical aperture 1.4) to obtain a high-resolution image of individual cilia (inset, Fig. 4a). The fraction of each cell type is calculated by dividing the area of the fluorescence of each cell type on the apical side by the total area of the image.

251

252

253

254

255

256

257

258

237

238

239

240

241

242

243

244

245

246

247

248

249

250

To prepare the culture for cross-section imaging (**Fig. S2**), following differentiation at ALI Day 28, we wash HBECs three times with PBS, warm the culture to 37°C, and fix the culture in 10% (v/v) neutral buffered formalin (VWR, 10015-196) for 24 hours. The culture is embedded into paraffin wax before 3 µm sections are cut. We use xylene (ThermoFisher, 396931000) to thoroughly deparaffinize sections, after which the xylene is removed using 100% ethanol. Then, we hydrate the sections through a graded series of ethanol (95%, 80%, and 70%) before washing twice in water. For antigen retrieval, we place slides in 500 ml of Antigen Retrieval Buffer (Bio-

Rad, HIS003B) and microwave the sections for 15 minutes. The immunostaining of acetylated-tubulin for ciliated cell, MUC5AC for goblet cells, and DAPI staining of cell nuclei is identical to the methods described above.

Transepithelial electric resistance (TEER) measurement. We measure TEER using an EVOM2 epithelial voltohmmeter (World Precision Instruments, Sarasota, FL). Before each measurement, we sterilize the electrodes with 70% ethanol, rinse them using sterilized DI water, and dry them. For each culture, we add 100 μL of DPBS to the apical side of the Transwell[®] to form an electrical circuit with the liquid in the basal chamber. We first measure the electric resistance of a blank Transwell[®] with or without gel coating. To measure the electric resistance across the HBEC culture, we gently place the electrodes into the medium on both the apical and basal sides of the cell culture without disrupting the cell surface. To obtain TEER for HBECs, the measured resistance is subtracted by the value of a blank Transwell[®] with or without gel and multiplied by the area of Transwell[®]. The measurements are performed on ALI days 1, 2, 3, 4, 5, 6, 7, 14, 21, and 28 to quantify the dependence of TEER values on culture time.

Quantification of HBEC migration and cell density. To monitor the migration of HBECs, we use a confocal microscope equipped with a 10x dry objective to acquire phase contrast images. The phase contrast mode allows for detecting the differences in the refractive index of cell body and junction, enabling label-free imaging of HBECs at their natural state. Moreover, the confocal microscope is equipped with an environmental chamber with temperature, CO₂, and humidity control to allow for long time imaging. For each condition, we image HBECs at 1 frame/min for 60 min on ALI days 7, 14, and 21. We use particle imaging velocimetry (PIV) to quantify the

282	velocity fields associated with collective cell migration (43). Interrogation windows of 64×64
283	pixels with 50% overlap are used; this window size allows for a spatial resolution of ~16 pixels
284	(9 μm).
285	
286	To measure cell density, for a randomly selected ROI, we count the number of cells manually
287	For cells on the four borders of the ROI, only cells on the upper and left borders are included
288	The cell density is calculated as the total number of cells divided by the area of ROI. For all the
289	measurements, we use cells from 4-6 normal donors to ensure sufficiently powered statistics.
290	
291	Measurement of the cell shape index. The cell shape index is defined as $S = P/\sqrt{A}$, where P is
292	the cell perimeter and A is the cell area. The cell contour is manually outlined based on the phase
293	contrast images. We use ImageJ to trace the cell contour to measure the cell perimeter and area
294	to calculate the cell shape index. For each condition, we randomly choose 100 cells from 5 wells
295	representing 5 normal donors to ensure sufficiently powered statistics.
296	
297	Statistical analysis. Statistical analysis is performed using the one-way analysis of variance
298	(ANOVA) method, which is followed by Tukey's Honest Significant Difference (HSD) test to
299	determine the significance of differences between pairs of group means. Curves in Fig 2b are
300	statistically compared at all timepoints (0, 2, 4,, 60 minutes) using Student's t-test.
301	

3. Results

3.1 Design and fabrication of the gel-ALI system

We design the gel-ALI system by coating the classic ALI system with a thin layer of PAAm hydrogel. This approach represents perhaps the simplest yet unexplored method for mimicking tissue stiffness. We choose PAAm as the hydrogel coating because it has been extensively used as a substrate for studying cell mechanics (44). Moreover, it can be easily synthesized using a one-step free radical polymerization. In a typical synthesis, we fix the volume ratio between the acrylamide (AAm) monomer (40% w/v) solution and the crosslinking agent *N,N'*-methylenebisacrylamide (BIS) (2% w/v) solution at 1:1. The mixture is dissolved in DI water at a prescribed concentration. In the presence of the catalyst tetramethylethylenediamine (TEMED) and the initiator ammonium persulfate (APS), the precursor monomers polymerize to form a network, as illustrated in **Fig. 1c**. By varying the concentration of the AAm/BIS mixture, the stiffness of the PAAm gel can be tuned in a wide range from ~80 Pa to ~21 kPa, covering the stiffness of healthy (~1 kPa) and the upper limit of IPF (~16 kPa) lung tissues, as shown in **Fig. 1d**.

To fabricate the gel-ALI culture system, we apply a prescribed volume of the reaction mixture to the apical side of a Transwell® insert. The solution is covered by a customized coverslip that fits the insert. Moreover, the surface of the coverslip is hydrophobic; this avoids wetting-induced spreading of the precursor hydrogel solution, such that the thickness of the hydrogel can be precisely controlled. After the solution is cured for about 30 min, we gently remove the coverslip (**Fig. 1e**). To quantify the gel thickness, we premix the reaction mixture with fluorescein isothiocyanate (FITC)-labeled dextran and use confocal microscopy to measure the thickness of

the fluorescence region (Materials and Methods). This *in situ* polymerization process ensures seamless contact and strong adhesion between the soft hydrogel and the stiff plastic membrane; this is essential to prevent the delamination of the hydrogel and the leakage of cells during long-term cell culture.

3.2 Determine the gel thickness for efficient nutrient transport

In a gel-ALI culture, nutrients must transport through the hydrogel from the basal to the apical side to maintain cell growth. Thus, it is critical to determine the conditions for efficient mass transport through the gel. The transport is largely determined by diffusion, a process dependent on both the mesh size and the thickness of the hydrogel. The mesh size ξ of a hydrogel is largely determined by the gel shear modulus G, $\xi \approx (k_B T/G)^{1/3}$, in which k_B is Boltzmann constant and T is the absolute temperature (35, 45). Because the stiffness is determined by the target lung tissues, ξ is pre-determined: for the gel mimicking healthy lung tissue with $G \approx 1kPa$, $\xi_h \approx 16$ nm; by contrast, for the gel mimicking IPF disease with $G \approx 16$ kPa, $\xi_d \approx 6$ nm. Therefore, we seek to determine the gel thickness allowing for efficient nutrient transport.

We measure the time it takes for protein mimics to transport through a hydrogel layer of various thickness from $100~\mu m$ to $1000~\mu m$. We use 70~kDa dextran as the probe molecule, which is a branched polymer with a hydrodynamic diameter of 6.4 nm (8); this value is comparable to the size of albumin, the largest protein in culture media (46). Because dextran molecules are prone to concentrate onto the surface of the plastic membrane due to unspecific interactions, we measure the fluorescence intensity of regions >25 μm above the membrane to avoid the effects of concentrated dextran on measurements, as illustrated in **Fig. 2a**.

350

351

352

353

354

355

356

357

358

359

360

361

362

363

364

365

To describe the transport properties of the gel, we introduce the half-decay time τ , at which the fluorescence intensity of the gel decreases to 50% of the initial value. For 1 kPa gel, as the thickness increases from 100 μ m to 250 μ m, τ increases by nearly three times from 10 to 30 min, as shown by purple and green curves in Fig. 2b. Further increasing the gel thickness to 500 µm dramatically prolongs the value τ to nearly 60 min (black dashed line, Fig. 2b); this time is much longer than the typical nutrient supply rate required for optimal cell culture (47). As the gel thickness becomes 1000 µm, the intensity decreases to 75% of its initial value after one hour (red dotted line, Fig. 2b). These results confirm the understanding that thinner gels permit more efficient mass transport. Moreover, even for the 16 kPa gel, 100 µm thickness allows for relatively efficient mass transport with τ≈20 min, as evidenced by the fluorescence intensity profiles across the gel layer at different time scales (thick red dashed line in Fig. 2c). The determined optimum gel thickness, ~100 µm, for efficient mass transport is much smaller than 750 µm, the thickness used for the same PAAm hydrogel in a recently developed magnetic microboat ALI culture (37). Yet, our results are consistent with the existing understanding that in native tissues mammalian cells are typically located within 100-200 µm of blood vessels (48) and that in engineered tissues only cells up to a distance of 200 µm away from the media have access to sufficient nutrients (38).

366

367

368

369

370

To complement the studies on transport properties of gels based on the diffusion of protein mimics, we quantify the effects of gel coating on the electrical resistance of the porous plastic membrane. The electrical resistance reflects the ionic conductivity across the gel coated membrane; therefore, it provides an indirect assessment of the transport properties of the gel. We

start with determining the electrical resistance of the semipermeable membrane without gel coating, which has a value of $159\pm10~\Omega$ cm² that is consistent with literature data (5). When the gel is relatively thin of $100~\mu m$, the increase in electric resistance is very small, ~5% regardless of gel stiffness (**Fig. S1**). Collectively, our results show that $100~\mu m$ gel coating is thin enough for efficient nutrient transport.

3.3 Gel-ALI system allows HBECs to differentiate into pseudostratified epithelium

Despite the efficient transport of protein mimics, the ultimate test of the gel-ALI system is to examine whether HBECs can grow and differentiate into pseudostratified bronchial epithelium. To this end, we activate the surface of the hydrogel using sulfosuccinimidyl 6-(4'-azido-2'-nitrophenylamino)hexanoate (sulfo-SANPAH), such that the hydrogel surface can be conjugated with type IV collagen, a standard ECM protein for culturing primary HBECs (**Fig. 1e**) (2). Similar to the classical ALI culture, primary HBECs are plated and cultured by adding medium to both the apical and basal sides for about one week to reach >90% confluence. Afterward, HBECs are transitioned to ALI by removing the apical medium and maintaining medium on the basal side only. The cells are cultured for 4 weeks after which HBECs are expected to fully differentiate to pseudostratified epithelium (2).

We perform immunostaining to identify the population of cells cultured on substrates of various stiffness (Materials and Methods). As expected, for the control group without gel coating, HBECs fully differentiate into pseudostratified epithelium consisting of ciliated cells and mucus-secreting goblet cells, as shown by the fluorescence images for each cell type in Fig. 3a and cross-section of the ALI culture in Fig. S2. Quantitatively, for the control group the fraction of ciliated cells is $(29\pm17)\%$, whereas the fraction of goblet cells is $(13\pm8)\%$. These values are

consistent with literature data that for *in vitro* HBEC culture the fractions of ciliated and goblet cells, respectively, are about 30% and 10-15% (49, 50).

Similarly, HBECs differentiate into pseudostratified epithelium on gels of 1 kPa (**Fig. 3b**) and 16 kPa (**Fig. 3c**). Interestingly, regardless of gel coating, the fraction of ciliated cells is in the range of 30-40% (**Fig. 3d**). Moreover, the fraction of goblet cells is around 20% and there is no significant difference among substrates of various stiffnesses (**Fig. 3e**). The stained ciliated and goblet cells together account for about 50% of the whole cell population; the rest unstained ones are other cell types such as basal cells and club cells (51, 52).

In parallel, we quantify the transepithelial electrical resistance (TEER) of HBEC cultures, a well-established method used to monitor HBECs during their various stages of growth and differentiation (53). We subtract the contribution from the gel coated semipermeable membrane to obtain the TEER values for HBECs. Up to ALI Day 7 the HBEC TEER value increases nearly linearly from ~200 to 350 Ω cm², reflecting the proliferation of HBECs (**Fig. 3f**). After ALI Day 7, the TEER value slightly decreases and becomes stable beyond ALI Day 21, reflecting the complete differentiation of HBECs. Moreover, the plateau TEER value 329±33 Ω cm² is consistent with previously reported ones (5) for well differentiated HBECs with tight cell junctions (**Fig. 3f**). Taken together, our results show that gel-ALI allows HBECs to differentiate into pseudostratified epithelium.

3.4 Pathological substrate stiffness promotes cell migration

We exploit the gel-ALI system to study the migration of HBECs, a process critical to human airway remodeling (54). Three groups are explored: (i) control with the conventional plastic substrate, (ii) hydrogel with stiffness of 1 kPa matching that of healthy lung tissues, and (iii) hydrogel with stiffness of 16 kPa matching that of fibrotic lung tissues. For each group, we use cells from five normal donors to ensure sufficiently powered statistics. The difference in refractive indices between the cell junction and the cell body allows us to use phase-contrast microscopy to measure the migration of cells (Materials and Methods). And we measure cell migration on different ALI days up to 3 weeks, a typical period for basal cell differentiation, as shown by representative images in Fig. 4a and Movies S1-S3. Using particle image velocimetry (PIV) (43), we compute the velocity map of cells, as shown by the heat map in Fig. 4b and Movies S1-S3.

The effects of gel stiffness on cell migration become more pronounced as the number of ALI days increases. For example, on ALI day 7, there is no significant difference in cell migration speed regardless of substrate stiffness, as shown by the histograms on the left of **Fig. 4c**. However, on ALI day 14, despite no significant difference between control and 1 kPa gel in cell migration speed (~0.30 µm/min), the speed for HBECs on 16 kPa gel increases by nearly 4 times to 1.14 µm/min. Moreover, a similar trend is observed on ALI day 21, although HBECs on 1 kPa gel migrate slightly faster than the control, as shown by the histograms on the right of **Fig. 4c**. Yet, across 21 days, for the control and 1 kPa gel, there is no significant difference in cell migration speed as the number of ALI days increases, as respectively shown by the gray and

green bars in **Fig. 4c**. By contrast, for the 16 kPa gel, cells exhibit a markedly high migration speed starting ALI day 14, as shown by the red bars in **Fig. 4c**.

Because the migration of cells in a confluent monolayer is known to be slower at a higher cell density (55, 56), we quantify the cell density under various substrate stiffness. For each cell culture, we count the number of cells per unit area and perform the same measurements for cells from five normal donors to ensure sufficiently powered statistics. We find no significant difference in cell density over the 21-day period, as shown in **Fig. 4d**. Moreover, the average cell density is $(3.2 \pm 0.2) \times 10^5/cm^2$, consistent with the previously reported value (49). These results preclude that the observed difference in cell migration speed is attributed to cell density.

To rationalize the difference in cell migration speed, we exploit a recently developed theoretical framework that correlates the migration of a confluent epithelial monolayer with cell shape (57, 58). The theory predicts that the cell shape index, $S = P/\sqrt{A}$, where P is the cell perimeter and A is the cell area, can be an indicator for cell migration. Below a threshold value $S_0 = 3.81$, cells are more round-like and are jammed, stationary; by contrast, for $S > S_0$, cells are more elongated and are unjammed, migratory. Consistent with this understanding, on the same ALI day there is no significant difference in S between cells cultured on the control and the 1 kPa gel on ALI day 7 and day 14; by contrast, for the pathologically relevant hydrogel of 16 kPa the value of S is significantly higher at 4.2 (**Fig. 4e**) on ALI day 14. Moreover, on ALI day 21 when the HBECs on the 1 kPa gel are nearly stationary, the cell shape index becomes 3.82, comparable to the threshold value S_0 , while the cell shape index of HBECs on 16 kPa is still significantly higher at 4.1 (**Fig. 4e**). These results indicate that hydrogel substrate of pathological stiffness promotes the

migration of HBECs at the air-liquid interface, highlighting the potential of the gel-ALI system for studying the effects of mechanical cues on fibrotic lung diseases.

4. Discussion and Conclusion

We have developed a gel-ALI culture system by coating a thin layer of polyacrylamide hydrogel onto the porous plastic membrane of the Transwell[®] insert of the classic ALI culture system. The hydrogel stiffness can be tuned in a wide range to precisely match that of the healthy and fibrotic lung tissues. The higher gel stiffness (16 kPa) explored in our gel-ALI system represents the upper limit of IPF lung tissues. To allow efficient nutrient transport, the hydrogel must be relatively thin at ~100 μm, significantly lower than the 750 μm gel thickness in a recently reported magnetic hydrogel boat-based ALI system (37). We show that the gel-ALI system allows primary HBECs to fully differentiate into pseudostratified epithelium, capturing essential biological features of human airway tissues *in vivo*.

Using the gel-ALI system, we study the effects of substrate stiffness on the migration of HBECs, a process critical to human airway remodeling. Moreover, we discover that hydrogel substrates of pathologically relevant stiffness promote the migration of HBECs at air-liquid interface; this represents a previously unrecognized phenomenon but can be rationalized in the context of a theoretical framework that associates jamming/unjamming transition of a confluent epithelial layer to the cell shape index. Moreover, our findings are consistent with existing *in vivo* results that airway epithelium undergoes fast migration in inflammatory airway diseases (59).

We note that our results show negligible difference in both the differentiation and migration of between HBECs on the extremely stiff substrate ($\sim 10^9$ Pa) and those on the hydrogel with

stiffness 1 kPa comparable to the healthy lung tissue. This behavior contrasts to that have been established for stem cell differentiation, in which stiffer substrates induces preferential osteogenesis over adipogenesis of mesenchymal stem cells (60). Additionally, recent studies reveal that cells often migrate faster on stiffer substrate unless beyond physiologically relevant stiffness (61). A possible explanation to our discovered conundrum is that the stiffness of the plastic membrane dramatically exceeds both the physiological stiffness of normal lungs and pathological stiffness of fibrotic lung tissues, so that HBECs cannot tell the difference between the plastic membrane and the hydrogel substrate with healthy lung tissue stiffness. Yet, the HBECs are able to distinguish the difference between hydrogels with physiologically and pathologically relevant stiffness. However, the exact mechanism for airway basal stem cell differentiation on hydrogel substrates with tissue-mimicking stiffness has yet to be elucidated, and our gel-ALI system may provide an approach to do so.

In the context of cell migration, our measurements are restricted to apical cells. However, typically at relatively long time >3 weeks, ALI cultures develop multiple layers in which a differentiated apical layer is on top of basal cells (62) (Fig. S2). Moreover, a recent study reveals that during an unjamming transition induced by mechanical compression or irradiation, compared to apical cells, basal cells exhibit a more elongated and enlarged morphology (62). Thus, an open question is whether the migration of apical cells is independent of basal cells. Answering this question requires simultaneously distinguishing and measuring the migration of apical and basal cells in a well differentiated live HBEC culture, which represents a technical challenge. However, one can partially address this question by measuring the migration of basal cells while they are maintained in the submerged culture before differentiation begins. We find

that there is no significant difference in the migration speed and cell shape index of basal cells over 7 days (**Fig. S3**, **Movies S4-6**). Beyond this period, the cells become confluent and need to transition to ALI culture. In addition to the observed negligible difference in apical cell migration, regardless of substrate stiffness on ALI Day 7 when it can be assumed to be a single layer of basal cells, our results suggest that basal cell migration is likely not affected by the hydrogel substrate. The enhanced migration speed of apical cells, starting from ALI Day 14, is likely not driven by underlying basal cells, and the unjamming of apical cells on the pathologically relevant stiff substrate takes time to occur.

Compared to the recently developed microfluidics-based (63) or magnetic hydrogel boat-based (37) ALI systems that rely on sophisticated microfabrication that often is not accessible to biological laboratories, our gel-ALI system is built on the classic, commercially available ALI system that has been widely used in biological laboratories. In addition, the polyacrylamide hydrogel chemistry is well established, and the fabrication process is facile and does not require any sophisticated instrument. Yet, polyacrylamide hydrogel is pure elastic so that the stiffness does not change over time; by contrast, the human lung tissue is a viscoelastic material with time-dependent mechanical properties (64). Integrating another polymer network such as alginate into the polyacrylamide hydrogel can result in a double-network hydrogel (65–67); this would enable controlling not only hydrogel stiffness but also relaxation time to mimic the dynamic nature of biological tissues, which are being increasingly recognized to be critical to fundamental cellular processes (64). Finally, the gel-ALI system is not restricted to culturing HBECs; instead, it should be general and applicable to small airway cells, which are more relevant to fibrotic lung diseases (28, 68, 69). In addition, the gel-ALI platform may be applied

to culturing intestinal epithelial cells (70) to study the effects of fibrosis on intestinal epithelial cells in the context of inflammatory bowel diseases (71, 72). Thus, we believe that the developed gel-ALI system represents perhaps the simplest yet versatile platform for studying the roles of pathologically relevant mechanical cues in human airway biology and diseases.

Acknowledgments: L.H.C. acknowledges the support from NSF (CAREER DMR-1944625). K.O. acknowledges the support by the National Heart, Lung, and Blood Institute (R01HL163602), the Cystic Fibrosis Foundation (OKUDA20G0), and a research grant from the Cystic Fibrosis Research Institute. We thank Dr. Richard Boucher at UNC Chapel Hill for critical reviewing the manuscript prior to submission. We thank Dr. Gang Chen, Dr. Camille Ehre, and Dr. Lin Sun at UNC Chapel Hill for helpful discussions on airway biology, Dr. Chongzhi Zang from UVA for discussions on statistical analysis, and Dr. Alison Criss from UVA for the assistance with the TEER measurements.

Author contributions: L.H.C., Z.J.H, and C.C. designed the research. Z.J.H. developed the protocol to fabricate the gel-ALI system. Z.J.H. and C.C performed rheological measurements of gel stiffness and analysis. C.C measured the gel transport properties. Z.J.H and R.D cultured HBECs on gel-ALI and performed immunostaining. C.C cultured HBECs on gel-ALI and measured the cell migration speed, the cell density, and the cell shape index. K.O. provided HBE cells and critical insights into the implications of gel-ALI system. L.H.C., Z.J.H., and C.C. wrote the paper. All authors reviewed and commented on the paper. L.H.C. conceived and supervised the study.

- 553 Competing interests: L.H.C., Z.J.H., and C.C. have filed a provisional patent application for the
- gel-ALI system.
- 555

<i>-</i>	TD C	
556	References	ď
<i>JJ</i> U	IXCICI CHCC	3

- 557 1. Wu R, Sato GH, Whitcutt MJ. Developing differentiated epithelial cell cultures: Airway
- epithelial cells. In: *Toxicological Sciences*. 1986, p. 580–590.
- 559 2. Fulcher ML, Gabriel S, Burns KA, Yankaskas JR, Randell SH. Well-differentiated
- human airway epithelial cell cultures. *Methods Mol Med* 107: 183–206, 2005. doi:
- 561 10.1385/1-59259-861-7:183.
- 562 3. Pezzulo AA, Starner TD, Scheetz TE, Traver GL, Tilley AE, Harvey BG, Crystal RG,
- McCray PB, Zabner J. The air-liquid interface and use of primary cell cultures are
- important to recapitulate the transcriptional profile of in vivo airway epithelia. Am J
- 565 *Physiol Lung Cell Mol Physiol* 300: 25–31, 2011. doi: 10.1152/ajplung.00256.2010.
- 566 4. Dvorak A, Tilley AE, Shaykhiev R, Wang R, Crystal RG. Do airway epithelium air-
- liquid cultures represent the in vivo airway epithelium transcriptome? Am J Respir Cell
- 568 *Mol Biol* 44: 465–473, 2011. doi: 10.1165/rcmb.2009-0453OC.
- 5. Leung C, Wadsworth SJ, Jasemine Yang S, Dorscheid DR. Structural and functional
- variations in human bronchial epithelial cells cultured in air-liquid interface using
- different growth media. *Am J Physiol Lung Cell Mol Physiol* 318: L1063–L1073, 2020.
- 572 doi: 10.1152/AJPLUNG.00190.2019.
- 573 6. **Baldassi D**, **Gabold B**, **Merkel OM**. Air-Liquid Interface Cultures of the Healthy and
- 574 Diseased Human Respiratory Tract: Promises, Challenges, and Future Directions. Adv
- 575 NanoBiomed Res 1: 2000111, 2021. doi: 10.1002/anbr.202000111.
- 576 7. Knowles MR, Boucher RC. Mucus clearance as a primary innate defense mechanism for
- 577 mammalian airways. *J Clin Invest* 109: 571–577, 2002. doi: Doi 10.1172/Jci200215217.
- 8. Button B, Cai L-H, Ehre C, Kesimer M, Hill DB, Sheehan JK, Boucher RC,

- Rubinstein M. A periciliary brush promotes the lung health by separating the mucus layer
- from airway epithelia. *Science* 337: 937–941, 2012. doi: 10.1126/science.1223012.
- 581 9. Hoang ON, Ermund A, Jaramillo AM, Fakih D, French CB, Flores JR, Karmouty-
- Quintana H, Magnusson JM, Fois G, Fauler M, Frick M, Braubach P, Hales JB,
- Kurten RC, Panettieri R, Vergara L, Ehre C, Adachi R, Tuvim MJ, Hansson GC,
- Dickey BF. Mucins MUC5AC and MUC5B Are Variably Packaged in the Same and in
- Separate Secretory Granules. Am J Respir Crit Care Med 206: 1081–1095, 2022. doi:
- 586 10.1164/rccm.202202-0309OC.
- 587 10. Roy MG, Livraghi-Butrico A, Fletcher AA, McElwee MM, Evans SE, Boerner RM,
- Alexander SN, Bellinghausen LK, Song AS, Petrova YM, Tuvim MJ, Adachi R,
- Romo I, Bordt AS, Bowden MG, Sisson JH, Woodruff PG, Thornton DJ, Rousseau
- K, De la Garza MM, Moghaddam SJ, Karmouty-Quintana H, Blackburn MR,
- Drouin SM, Davis CW, Terrell KA, Grubb BR, O'Neal WK, Flores SC, Cota-Gomez
- A, Lozupone CA, Donnelly JM, Watson AM, Hennessy CE, Keith RC, Yang I V,
- Barthel L, Henson PM, Janssen WJ, Schwartz DA, Boucher RC, Dickey BF, Evans
- 594 CM. Muc5b is required for airway defence. *Nature* 505: 412–6, 2014. doi:
- 595 10.1038/nature12807.
- 596 11. Park JA, Sharif AS, Tschumperlin DJ, Lau L, Limbrey R, Howarth P, Drazen JM.
- Tissue factor-bearing exosome secretion from human mechanically stimulated bronchial
- epithelial cells in vitro and in vivo. J Allergy Clin Immunol 130: 1375–1383, 2012. doi:
- 599 10.1016/j.jaci.2012.05.031.
- 12. Tschumperlin DJ, Dal G, Maly I V., Kikuchi T, Lalho LH, McVittie AK, Haley KJ,
- 601 Lilly CM, So PTC, Lauffenburger DA, Kamm RD, Drazen JM. Mechanotransduction

- through growth-factor shedding into the extracellular space. *Nature* 429: 83–86, 2004. doi:
- 603 10.1038/nature02543.
- 13. Jakiela B, Brockman-Schneider R, Amineva S, Lee WM, Gern JE. Basal cells of
- differentiated bronchial epithelium are more susceptible to rhinovirus infection. Am J
- 606 Respir Cell Mol Biol 38: 517–523, 2008. doi: 10.1165/rcmb.2007-0050OC.
- 607 14. Michi AN, Proud D. A toolbox for studying respiratory viral infections using air-liquid
- interface cultures of human airway epithelial cells. Am J Physiol Lung Cell Mol Physiol
- 609 321: 263–279, 2021. doi: 10.1152/AJPLUNG.00141.2021.
- 610 15. **Boucher RC**. Muco-obstructive lung diseases. *NEJM* 380: 1941–1953, 2019. doi:
- 611 10.1056/NEJMra1813799.
- 612 16. Han MLK, Agusti A, Calverley PM, Celli BR, Criner G, Curtis JL, Fabbri LM,
- Goldin JG, Jones PW, MacNee W, Make BJ, Rabe KF, Rennard SI, Sciurba FC,
- 614 Silverman EK, Vestbo J, Washko GR, Wouters EFM, Martinez FJ. Chronic
- obstructive pulmonary disease phenotypes: The future of COPD. Am J Respir Crit Care
- 616 *Med* 182: 598–604, 2010. doi: 10.1164/rccm.200912-1843CC.
- 617 17. M. Rowe, steven; M.D., Stacey Miller, B.S., and Eric J. Sorscher M. Cystic fibrosis
- [Online]. NEJM 352: 1992–2001, 2015. https://www.erswhitebook.org/chapters/cystic-
- fibrosis/%0Awww.informahealthcare.com.
- 620 18. Henderson AG, Ehre C, Button B, Abdullah LH, Cai L-H, Leigh MW, DeMaria GC,
- Matsui H, Donaldson SH, Davis CW, Sheehan JK, Boucher RC, Kesimer M. Cystic
- fibrosis airway secretions exhibit mucin hyperconcentration and increased osmotic
- 623 pressure. J Clin Invest 124: 3047–3060, 2014. doi: 10.1172/JCI73469.
- 624 19. Knowles MR, Zariwala M, Leigh M. Primary Ciliary Dyskinesia. Clin Chest Med 37:

- 625 449–461, 2016. doi: 10.1016/j.ccm.2016.04.008.
- 626 20. Gras D, Bourdin A, Vachier I, De Senneville L, Bonnans C, Chanez P. An ex vivo
- model of severe asthma using reconstituted human bronchial epithelium. J Allergy Clin
- 628 *Immunol* 129: 1259-1266.e1, 2012. doi: 10.1016/j.jaci.2012.01.073.
- 629 21. Burgstaller G, Oehrle B, Gerckens M, White ES, Schiller HB, Eickelberg O. The
- instructive extracellular matrix of the lung: Basic composition and alterations in chronic
- 631 lung disease. Eur Respir J 50, 2017. doi: 10.1183/13993003.01805-2016.
- 632 22. Zhou Y, Horowitz JC, Naba A, Ambalavanan N, Atabai K, Balestrini J, Bitterman
- PB, Corley RA, Ding B Sen, Engler AJ, Hansen KC, Hagood JS, Kheradmand F, Lin
- QS, Neptune E, Niklason L, Ortiz LA, Parks WC, Tschumperlin DJ, White ES,
- 635 Chapman HA, Thannickal VJ. Extracellular matrix in lung development, homeostasis
- and disease. *Matrix Biol* 73: 77–104, 2018. doi: 10.1016/j.matbio.2018.03.005.
- 637 23. Williams AH, Hebert AM, Boehm RC, Huddleston ME, Jenkins MR, Velev OD,
- Nelson MT. Bioscaffold Stiffness Mediates Aerosolized Nanoparticle Uptake in Lung
- Epithelial Cells. ACS Appl Mater Interfaces 13: 50643–50656, 2021. doi:
- 640 10.1021/acsami.1c09701.
- 641 24. Huang X, Yang N, Fiore VF, Barker TH, Sun Y, Morris SW, Ding Q, Thannickal VJ,
- **Zhou Y.** Matrix stiffness-induced myofibroblast differentiation is mediated by intrinsic
- 643 mechanotransduction. Am J Respir Cell Mol Biol 47: 340–348, 2012. doi:
- 644 10.1165/rcmb.2012-0050OC.
- 645 25. White ES. Lung extracellular matrix and fibroblast function. Ann Am Thorac Soc 12:
- 646 S30–S33, 2015. doi: 10.1513/AnnalsATS.201406-240MG.
- 647 26. Liu F, Mih JD, Shea BS, Kho AT, Sharif AS, Tager AM, Tschumperlin DJ. Feedback

- amplification of fibrosis through matrix stiffening and COX-2 suppression. J Cell Biol
- 649 190: 693–706, 2010. doi: 10.1083/jcb.201004082.
- 650 27. De Hilster RHJ, Sharma PK, Jonker MR, White ES, Gercama EA, Roobeek M,
- Timens W, Harmsen MC, Hylkema MN, Burgess JK. Human lung extracellular matrix
- hydrogels resemble the stiffness and viscoelasticity of native lung tissue. Am J Physiol -
- 653 Lung Cell Mol Physiol 318: L698–L704, 2020. doi: 10.1152/AJPLUNG.00451.2019.
- 654 28. Booth AJ, Hadley R, Cornett AM, Dreffs AA, Matthes SA, Tsui JL, Weiss K,
- Horowitz JC, Fiore VF, Barker TH, Moore BB, Martinez FJ, Niklason LE, White ES.
- Acellular normal and fibrotic human lung matrices as a culture system for in vitro
- 657 investigation. Am J Respir Crit Care Med 186: 866–876, 2012. doi:
- 658 10.1164/rccm.201204-0754OC.
- 659 29. Liu F, Lagares D, Choi KM, Stopfer L, Marinković A, Vrbanac V, Probst CK,
- Hiemer SE, Sisson TH, Horowitz JC, Rosas IO, Fredenburgh LE, Feghali-Bostwick
- 661 C, Varelas X, Tager AM, Tschumperlin DJ. Mechanosignaling through YAP and TAZ
- drives fibroblast activation and fibrosis. Am J Physiol Lung Cell Mol Physiol 308: L344–
- 663 L357, 2015. doi: 10.1152/ajplung.00300.2014.
- 664 30. **Huh D Matthews B MAM-ZMHHID**. Reconstituting Organ-Level Lung. *Science* 328:
- 665 1662–1668, 2010.
- 666 31. Benam KH, Villenave R, Lucchesi C, Varone A, Hubeau C, Lee H-HH, Alves SE,
- Salmon M, Ferrante TC, Weaver JC, Bahinski A, Hamilton GA, Ingber DE. Small
- airway-on-a-chip enables analysis of human lung inflammation and drug responses in
- vitro. *Nat Methods* 13: 151–157, 2016. doi: 10.1038/nmeth.3697.
- 670 32. Huh D, Kim HJ, Fraser JP, Shea DE, Khan M, Bahinski A, Hamilton GA, Ingber

- **DE**. Microfabrication of human organs-on-chips. *Nat Protoc* 8: 2135–2157, 2013. doi:
- 672 10.1038/nprot.2013.137.
- 673 33. Cai L-H, Kodger TE, Guerra RE, Pegoraro AF, Rubinstein M, Weitz DA. Soft
- Poly(dimethylsiloxane) elastomers from architecture-driven entanglement free design. Adv
- 675 *Mater* 27: 5132–5140, 2015. doi: 10.1002/adma.201502771.
- 676 34. Guimarães CF, Gasperini L, Marques AP, Reis RL. The stiffness of living tissues and
- its implications for tissue engineering. *Nat Rev Mater* 5: 351–370, 2020. doi:
- 678 10.1038/s41578-019-0169-1.
- 679 35. Li J, Mooney DJ. Designing hydrogels for controlled drug delivery. Nat Rev Mater 1: 1–
- 680 18, 2016. doi: 10.1038/natrevmats.2016.71.
- 681 36. Caliari SR, Burdick JA. A practical guide to hydrogels for cell culture. *Nat Methods* 13:
- 682 405–414, 2016. doi: 10.1038/nmeth.3839.
- 683 37. Chandrasekaran A, Kouthouridis S, Lee W, Lin N, Ma Z, Turner MJ, Hanrahan JW,
- Moraes C. Magnetic microboats for floating, stiffness tunable, air-liquid interface
- 685 epithelial cultures. *Lab Chip* 19: 2786–2798, 2019. doi: 10.1039/c9lc00267g.
- 686 38. Rouwkema J, Koopman BFJM, Blitterswijk CAV, Dhert WJA, Malda J. Supply of
- nutrients to cells in engineered tissues. *Biotechnol Genet Eng Rev* 26: 163–178, 2009. doi:
- 688 10.5661/bger-26-163.
- 689 39. Estermann M, Spiaggia G, Septiadi D, Dijkhoff IM, Drasler B, Petri-Fink A, Rothen-
- Rutishauser B. Design of Perfused PTFE Vessel-Like Constructs for In Vitro
- 691 Applications. *Macromol Biosci* 21: 1–7, 2021. doi: 10.1002/mabi.202100016.
- 692 40. Sellgren KL, Butala EJ, Gilmour BP, Randell SH, Grego S. A biomimetic
- 693 multicellular model of the airways using primary human cells. *Lab Chip* 14: 3349–3358,

- 694 2014. doi: 10.1039/c4lc00552j.
- 695 41. Soloukhin VA, Brokken-Zijp JCM, Van Asselen OLJ, De With G. Physical aging of
- 696 polycarbonate: Elastic modulus, hardness, creep, endothermic peak, molecular weight
- distribution, and infrared data. *Macromolecules* 36: 7585–7597, 2003. doi:
- 698 10.1021/ma0342980.
- 699 42. Chaudhuri T, Rehfeldt F, Sweeney HL, Discher DE. Preparation of collagen-coated
- gels that maximize in vitro myogenesis of stem cells by matching the lateral elasticity of
- in vivo muscle. In: *Methods in Molecular Biology*, edited by Conboy IM, Schaffer D V,
- Barcellos-Hoff MH, Li S. Humana Press, p. 185–202.
- 703 43. Thielicke W, Sonntag R. Particle Image Velocimetry for MATLAB: Accuracy and
- enhanced algorithms in PIVlab. J Open Res Softw 9: 1–14, 2021. doi: 10.5334/JORS.334.
- 705 44. Kandow CE, Georges PC, Janmey PA, Beningo KA. Polyacrylamide Hydrogels for
- 706 Cell Mechanics: Steps Toward Optimization and Alternative Uses. *Methods Cell Biol* 83:
- 707 29–46, 2007. doi: 10.1016/S0091-679X(07)83002-0.
- 708 45. **Rubinstein M, Colby RH**. *Polymer Physics*. Oxford, UK: Oxford University Press, 2003.
- 709 46. Francis GL. Albumin and mammalian cell culture: Implications for biotechnology
- 710 applications. *Cytotechnology* 62: 1–16, 2010. doi: 10.1007/s10616-010-9263-3.
- 711 47. Glacken MW. Catabolic Control of Mammalian Cell Culture. Bio/Technology 6: 1041–
- 712 1050, 1988. doi: 10.1038/nbt0988-1041.
- 713 48. Carmeliet P, Jain RK. Angiogenesis in cancer and other diseases [Online]. *Nature* 407:
- 714 249–257, 2000. www.nature.com.
- 715 49. Mercer RR, Russell ML, Roggli VL, Crapo JD. Cell number and distribution in human
- 716 and rat airways. *Am J Respir Cell Mol Biol* 10: 613–624, 1994. doi:

- 717 10.1165/ajrcmb.10.6.8003339.
- 718 50. Boers JE, Ambergen AW, Thunnissen FBJM. Number and proliferation of Clara cells
- 719 in normal human airway epithelium. *Am J Respir Crit Care Med* 67: 1585–1591, 2012.
- 720 doi: 10.1164/ajrccm.159.5.9806044.
- 721 51. Deprez M, Zaragosi LE, Truchi M, Becavin C, García SR, Arguel MJ, Plaisant M,
- Magnone V, Lebrigand K, Abelanet S, Brau F, Paquet A, Pe'er D, Marquette CH,
- Leroy S, Barbry P. A single-cell atlas of the human healthy airways. Am J Respir Crit
- 724 *Care Med* 202: 1636–1645, 2020. doi: 10.1164/rccm.201911-2199OC.
- 725 52. **Davis JD**, **Wypych TP**. Cellular and functional heterogeneity of the airway epithelium.
- 726 *Mucosal Immunol* 14: 978–990, 2021. doi: 10.1038/s41385-020-00370-7.
- 53. Srinivasan B, Kolli AR, Esch MB, Abaci HE, Shuler ML, Hickman JJ. TEER
- Measurement Techniques for In Vitro Barrier Model Systems. *J Lab Autom* 20: 107–126,
- 729 2015. doi: 10.1177/2211068214561025.
- 730 54. Fredberg J, Mitchel J, Kim JH, Park J. Unjamming and cell shape in the asthmatic
- 731 airway epithelium. *FASEB J* 30: 2016.
- 732 55. Rosen P, Misfeldt DS. Cell density determines epithelial migration in culture. Proc Natl
- 733 Acad Sci USA 77: 4760–4763, 1980. doi: 10.1073/pnas.77.8.4760.
- 734 56. Poujade M, Grasland-Mongrain E, Hertzog A, Jouanneau J, Chavrier P, Ladoux B,
- 735 **Buguin A**, **Silberzan P**. Collective migration of an epithelial monolayer in response to a
- 736 model wound. *Proc Natl Acad Sci USA* 104: 15988–15993, 2007. doi:
- 737 10.1073/pnas.0705062104.
- 738 57. Park J-A, Kim JH, Bi D, Mitchel JA, Qazvini NT, Tantisira K, Park CY, McGill M,
- Kim S-H, Gweon B, Notbohm J, Steward Jr R, Burger S, Randell SH, Kho AT,

- Tambe DT, Hardin C, Shore SA, Israel E, Weitz DA, Tschumperlin DJ, Henske EP,
- Weiss ST, Manning ML, Butler JP, Drazen JM, Fredberg JJ. Unjamming and cell
- shape in the asthmatic airway epithelium. *Nat Mater* 14: 1040–1048, 2015. doi:
- 743 10.1038/nmat4357.
- 744 58. Atia L, Bi D, Sharma Y, Mitchel JA, Gweon B, Koehler SA, Decamp SJ, Lan B, Kim
- JH, Hirsch R, Pegoraro AF, Lee KH, Starr JR, Weitz DA, Martin AC, Park JA,
- Rutler JP, Fredberg JJ. Geometric constraints during epithelial jamming. *Nat Phys* 14:
- 747 613–620, 2018. doi: 10.1038/s41567-018-0089-9.
- 748 59. Erjefält JS, Erjefält I, Sundler F, Persson CGA. In vivo restitution of airway
- 749 epithelium. *Cell Tissue Res* 281: 305–316, 1995. doi: 10.1007/BF00583399.
- 750 60. Engler AJ, Sen S, Sweeney HL, Discher DE. Matrix elasticity directs stem cell lineage
- 751 specification. *Cell* 126: 677–689, 2006. doi: 10.1016/j.cell.2006.06.044.
- 752 61. Bangasser BL, Shamsan GA, Chan CE, Opoku KN, Tüzel E, Schlichtmann BW,
- Kasim JA, Fuller BJ, McCullough BR, Rosenfeld SS, Odde DJ. Shifting the optimal
- stiffness for cell migration. *Nat Commun* 8: 1–10, 2017. doi: 10.1038/ncomms15313.
- 755 62. Phung T-KN, Mitchel JA, O'Sullivan MJ, Park J-A. Quantification of basal stem cell
- elongation and stress fiber accumulation in the pseudostratified airway epithelium during
- 757 the unjamming transition. *Biol Open* 12: bio059727, 2023. doi: 10.1242/bio.059727.
- 758 63. Zheng L, Dong H, Zhao W, Zhang X, Duan X, Zhang H, Liu S, Sui G. An Air-Liquid
- 759 Interface Organ-Level Lung Microfluidics Platform for Analysis on Molecular
- Mechanisms of Cytotoxicity Induced by Cancer-Causing Fine Particles. ACS Sensors 4:
- 761 907–917, 2019. doi: 10.1021/acssensors.8b01672.
- 762 64. Chaudhuri O, Cooper-White J, Janmey PA, Mooney DJ, Shenoy VB. Effects of

- extracellular matrix viscoelasticity on cellular behaviour. *Nature* 584: 535–546, 2020. doi:
- 764 10.1038/s41586-020-2612-2.
- 765 65. **Gong JP**. Why are double network hydrogels so tough? *Soft Matter* 6: 2583–2590, 2010.
- 766 doi: 10.1039/b924290b.
- 767 66. Sun J-Y, Zhao X, Illeperuma WRKK, Chaudhuri O, Oh KH, Mooney DJ, Vlassak JJ,
- Suo Z. Highly stretchable and tough hydrogels. *Nature* 489: 133–136, 2012. doi:
- 769 10.1038/nature11409.
- 770 67. Zhu J, He Y, Wang Y, Cai L-H. Voxelated bioprinting of modular double-network bio-
- ink droplets. .
- Okuda K, Dang H, Kobayashi Y, Carraro G, Nakano S, Chen G, Kato T, Asakura T,
- Gilmore RC, Morton LC, Lee RE, Mascenik T, Yin WN, Cardenas SMB, O'Neal YK,
- Minnick CE, Chua M, Quinney NL, Gentzsch M, Anderson CW, Ghio A, Matsui H,
- Nagase T, Ostrowski LE, Grubb BR, Olsen JC, Randell SH, Stripp BR, Tata PR,
- 776 **O'Neal WK**. Secretory cells dominate airway CFTR expression and function in human
- airway superficial epithelia. *Am J Respir Crit Care Med* 203: 1275–1289, 2021. doi:
- 778 10.1164/rccm.202008-3198OC.
- 779 69. Ikezoe K, Hackett TL, Peterson S, Prins D, Hague CJ, Murphy D, LeDoux S, Chu F,
- 780 Xu F, Cooper JD, Tanabe N, Ryerson CJ, Pare PD, Coxson HO, Colby T V., Hogg
- JC, Vasilescu DM. Small airway reduction and fibrosis is an early pathologic feature of
- 782 idiopathic pulmonary fibrosis. Am J Respir Crit Care Med 204: 1048–1059, 2021. doi:
- 783 10.1164/rccm.202103-0585OC.
- 784 70. Ootani A, Li X, Sangiorgi E, Ho QT, Ueno H, Toda S, Sugihara H, Fujimoto K,
- Weissman IL, Capecchi MR, Kuo CJ. Sustained in vitro intestinal epithelial culture

786		within a Wnt-dependent stem cell niche. <i>Nat Med</i> 15: 701–706, 2009. doi:
787		10.1038/nm.1951.
788	71.	Stidham RW, Xu J, Johnson LA, Kim K, Moons DS, McKenna BJ, Rubin JM,
789		Higgins PDR. Ultrasound elasticity imaging for detecting intestinal fibrosis and
790		inflammation in rats and humans with Crohn's disease. Gastroenterology 141: 819-826
791		2011. doi: 10.1053/j.gastro.2011.07.027.
792	72.	Johnson LA, Rodansky ES, Sauder KL, Horowitz JC, Mih JD, Tschumperlin DJ,
793		Higgins PD. Matrix stiffness corresponding to strictured bowel induces a fibrogenic
794		response in human colonic fibroblasts. Inflamm Bowel Dis 19: 891–903, 2013. doi:
795		10.1097/MIB.0b013e3182813297.
796		
797		

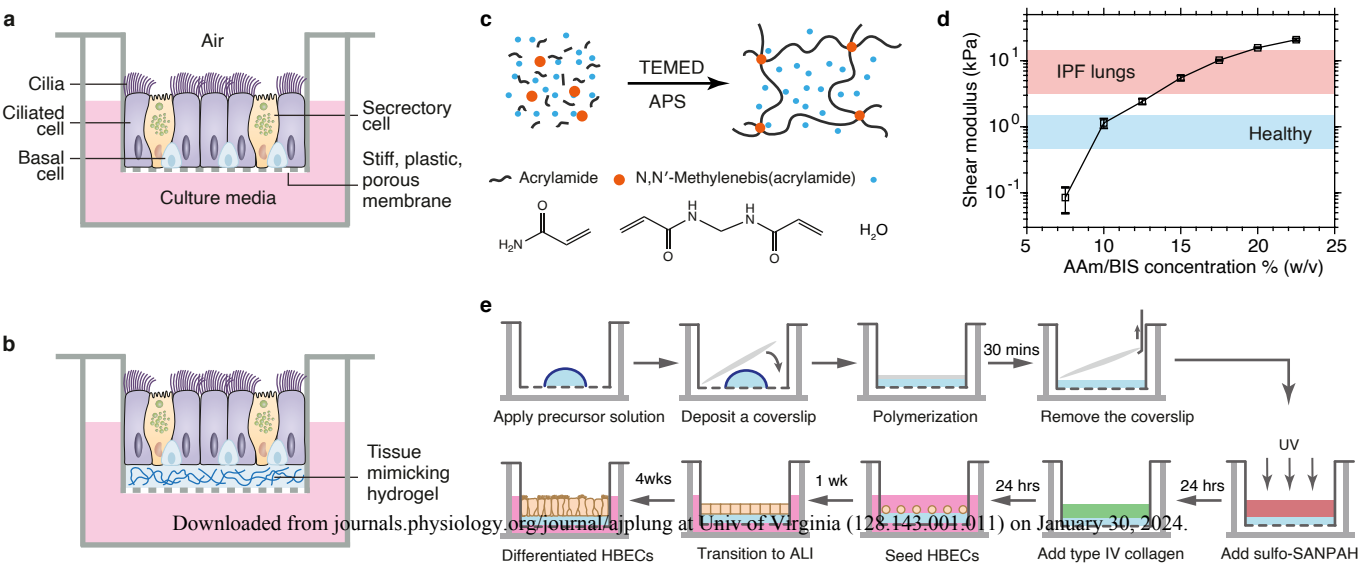
T-10	▼	•
Figure	Legen	ds

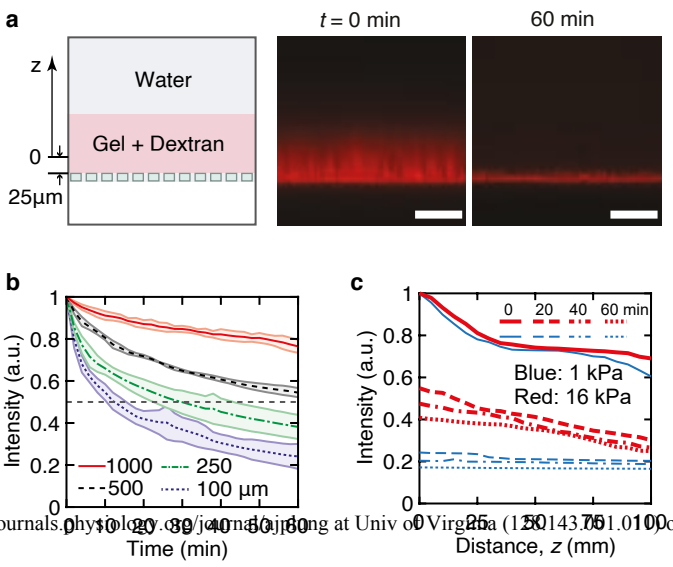
Figure 1. Design and fabrication of the gel-ALI culture system. (a) In a conventional ALI system, HBECs are cultured on a stiff, porous plastic membrane with a fixed stiffness on the order of 10^9 Pa. (b) In a gel-ALI system, HBECs are cultured on a layer of porous hydrogel with tunable stiffness matching that of lung tissues. (c) PAAm hydrogel is formed by copolymerizing AAm monomers and crosslinking agent BIS in the presence of initiator APS and catalyst TEMED. (d) Dependence of the shear modulus of the hydrogel on the concentration of AAm/BIS mixture measured at 20 °C at a fixed strain of 0.5% and oscillatory shear frequency of 1 rad/sec. Light blue region: shear modulus of healthy lung tissues within the range of $\sim 0.6 - 1.5$ kPa; light red region: shear modulus of IPF lung tissues within the range of $\sim 3 - 16$ kPa. The stiffness of IPF lung tissues often exhibits a large extent of heterogeneity with shear modulus ranging from 3 to 16 kPa (26–29). (e) Flowchart for the fabrication of PAAm hydrogel-coated ALI culture system.

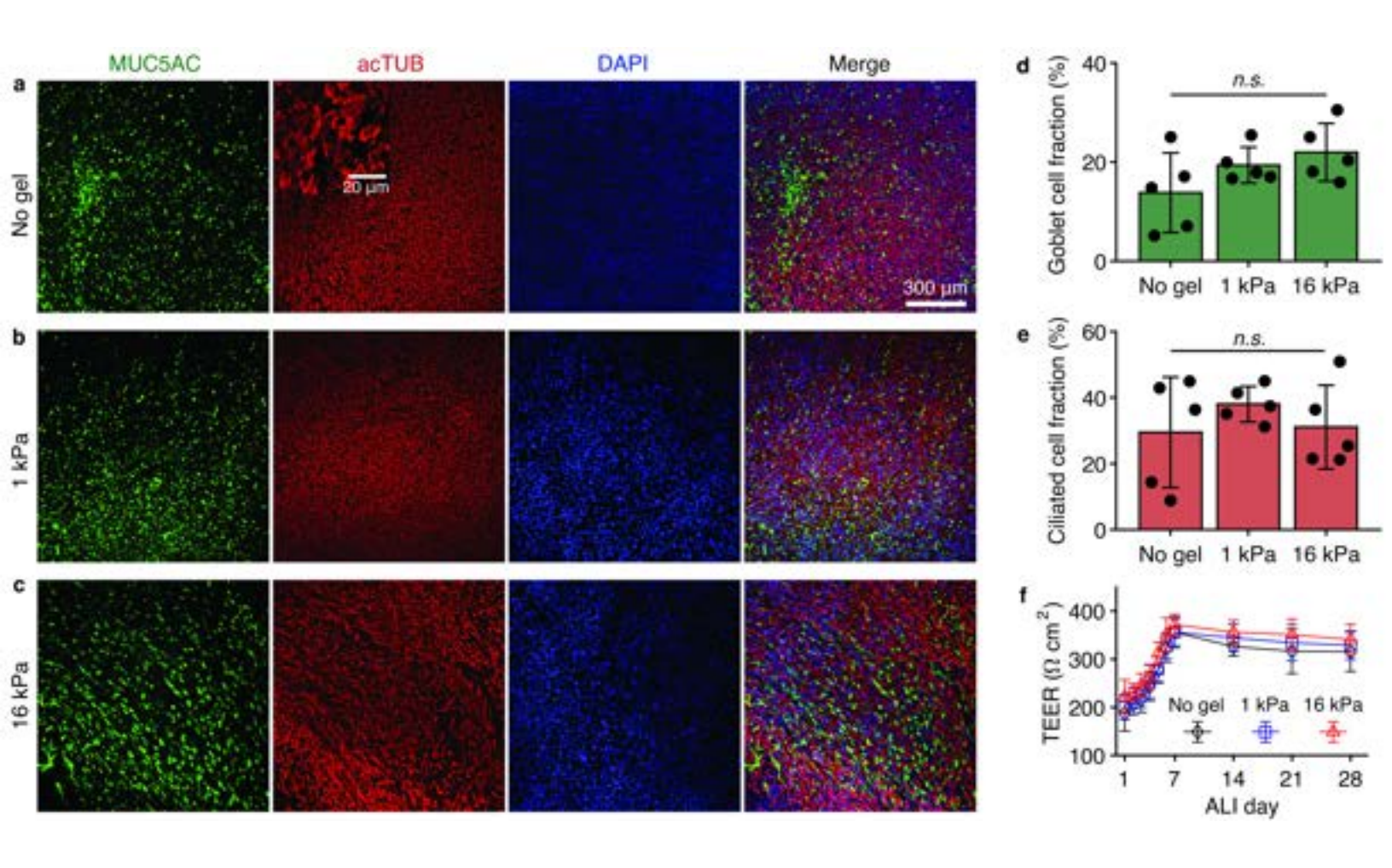
Figure 2. Transport properties of the gel-ALI system. (a) A schematic of the experimental setup (left) for measuring the diffusion of FITC-dextran molecules out of the gel. Dextran is premixed with the precursor gel solution during fabrication. z, the distance away from the reference point, which is chosen to be 25 μ m above the porous membrane to avoid its effects on fluorescence intensity. Representative fluorescence images for 1 kPa gel of 100 μ m in thickness at 0 min (middle) and 60 min (right). (b) Dependence of the average fluorescence intensity of the gel layer of various thicknesses on waiting time: 1000 μ m (red solid line), 500 μ m (black dashed line), 250 μ m (green dash-dotted line), and 100 μ m (purple dotted line). The measurements are performed for the region at distance >25 μ m above the porous membrane. The shadowed zone represents with the width of standard deviation; n=3. The curves are statistically compared at all timepoints (0, 2, 4, ..., 60 minutes), and difference between curves is statistically significant at all timepoints except time 0. (c) Fluorescence intensity profiles of the gel layer at various waiting times for gels of 1 kPa (red) and 16 kPa (blue).

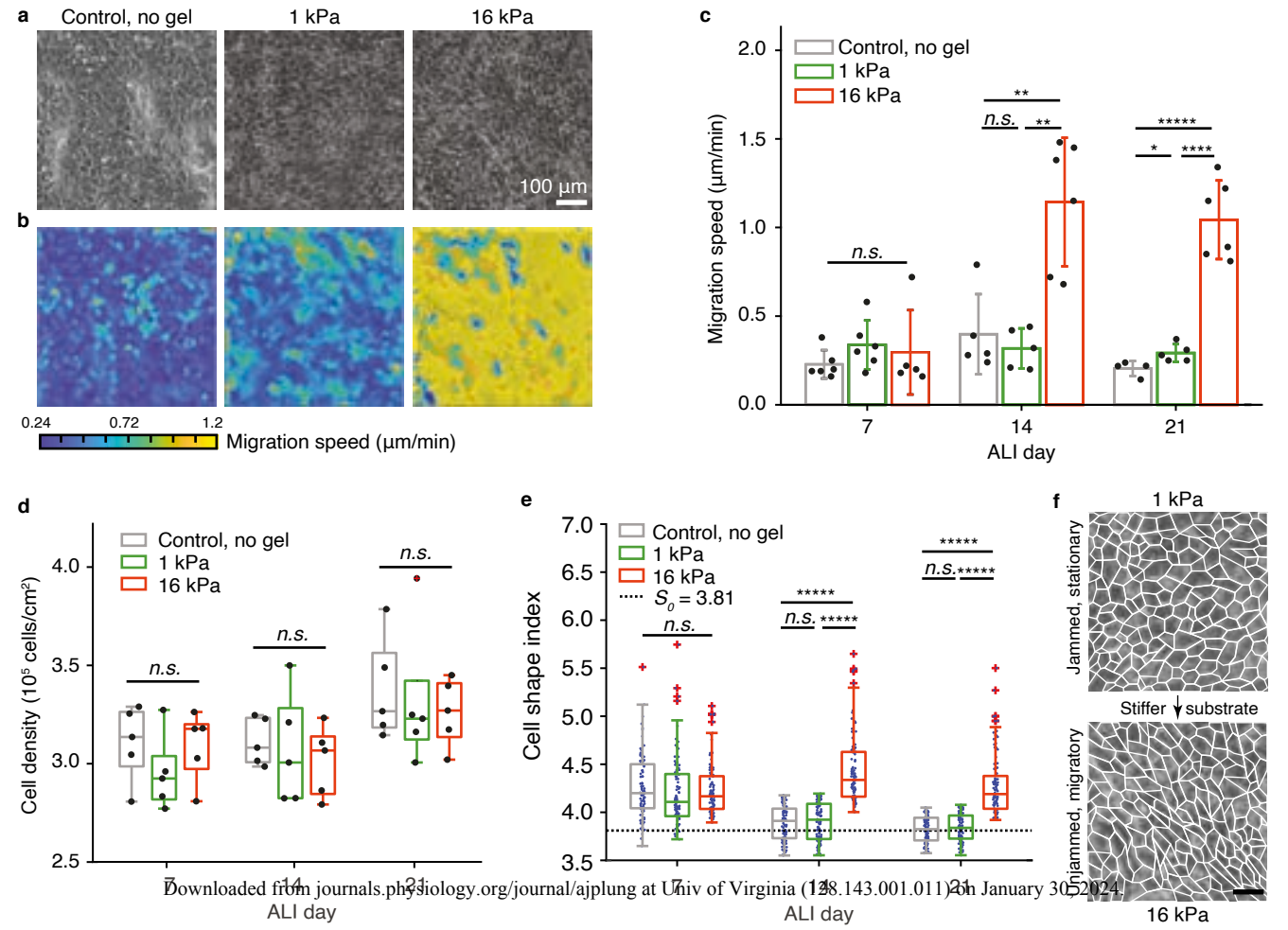
Figure 3. The gel-ALI system allows for HBECs differentiating into pseudostratified
epithelium. (a-c) Immunofluorescence staining of cells after ALI culture for 4 weeks: (a)
conventional ALI culture without gel coating, (b) ALI culture on 1 kPa gel, and (c) ALI culture
on 16 kPa gel. Green: MUC5AC/goblet cells; red: AcTUB/ciliated cells; blue: DAPI/nuclei.
Inset in (a): Zoom-in view of cilia. The fraction of (d) ciliated cells and (e) goblet cells on
substrates of various stiffnesses. (f) Transepithelial electrical resistance (TEER) of HBEC
cultures at different ALI days. $n.s.$, not significant. Values are mean \pm SD, $n = 5$ different donors.
One-way ANOVA is used for statistical analysis.

Figure 4. A stiffer substrate promotes migration of HBECs. (a) Example phase-contrast images of HBECs cultured on substrates of different stiffness on ALI day 21. (b) Speed maps for the migration of HBECs on substrates of different stiffness on ALI day 21. (c) Average cell migration speed, (d) density, and (e) cell shape index S of HBECs under different substrate stiffness on ALI days 7, 14, and 21. n.s.: not significant; *p < 0.05, **p < 0.01, **** p < 0.001, ***** p < 0.0001. For (c), values are mean \pm SD, n = 4-6 donors; for (d), n = 5 donors; for (e), n = 100 cells. One-way ANOVA is used for statistical analysis. In (d), the red data point is from one of the five donor samples and is considered as an outlier. (f) Substrates with pathological stiffness promote migration of cells by fluidizing jammed epithelia. Scale bar, $50 \, \mu m$,

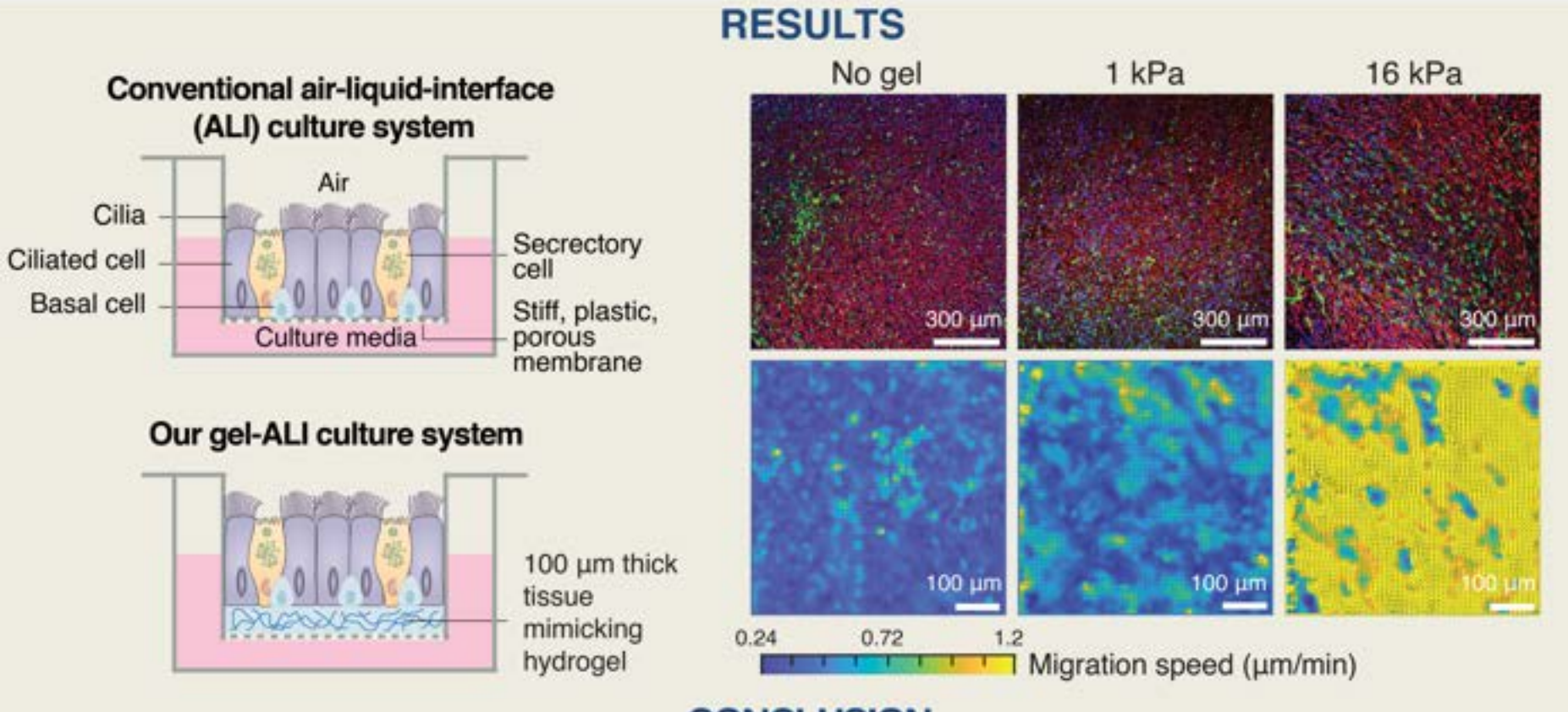








A gel-coated ALI system better captures human lung microenvironment



CONCLUSION

A gel-coated ALI culture system provides perhaps the simplest yet a versatile platform for studying the roles of pathologically relevant mechanical cues in human airway biology and diseases.